Stability of flexible orbital structures

Andra-Ana-Maria GHEORGHIU*[1,2], Cristian-Emil CONSTANTINESCU[2]

*Corresponding author
*,[1]INCAS - National Institute for Aerospace Research "Elie Carafoli",
B-dul Iuliu Maniu 220, Bucharest 061126, Romania,
gheorghiu.andra@incas.ro
[2]Faculty of Aerospace Engineering,
National University of Science and Technology POLITEHNICA Bucharest,
Gheorghe Polizu 1, 011061, Bucharest, Romania

DOI: 10.13111/2066-8201.2025.17.2.3

Received: 5 May 2025/ Accepted: 29 May 2025/ Published: June 2025

Abstract: *This paper presents the study of the stability of flexible orbital structures. The stability of the motion of space tether systems is analysed using methods that include mathematical models for solving equations. The selection of material for performing the simulations was important in order to reproduce the conditions in the Earth orbit as precisely as possible. A long cable configuration of space tether was analysed in the simulations. Comparisons between the structures were made, for various values of the elasticity and damping constants. Finally, an optimal configuration was chosen according to dynamic stability and endurance in the space environment.*

Key Words: *stability, flexible orbital structures, tether systems, mathematical model, dynamics*

1. INTRODUCTION

As space missions become more complex and diverse, the need for efficient, lightweight, and multifunctional systems has grown considerably. Space tethers provide effective solutions to the logistical and energy challenges encountered in both near-Earth and deep space missions. Space Tether Systems (STS) are mechanical structures consisting of orbital bodies linked by long, flexible tethers, often as long as or even longer than the bodies themselves. Unlike traditional spacecraft, STS feature extended structures, can change configuration by deploying or retracting tethers, and, when using conductive tethers, can interact electrodynamically with the space environment, such as Earth's magnetic field and ionosphere. Based on how they operate, STS can be divided into two main categories: static systems, where the parameters remain constant during operation (such as tether length, mass distribution, and relative positioning) and dynamic systems, characterized by the ability for active reconfiguration.

An STS is referred to as electrodynamic when it includes conductive tethers capable of generating or responding to induced currents through interaction with the geospatial environment, regardless of whether the system is static or dynamic [1].

An electrodynamic tether generates a current along its length that interacts with Earth's magnetic field to produce an electrodynamic force, which can be used to alter the characteristics of the initial orbit.

While all orbital elements can be influenced by this force, operationally, some change much more rapidly than others for a given tether current [2].

Space tether systems support various objectives, such as studies on tether propulsion [3], gravitational stabilization, and dynamics.

However, several technical challenges can arise during missions. These include the gravity gradient effect, which can cause tethers to maintain a vertical orientation due to slight gravitational variations along their length instead of rotating end-to-end [4], atomic oxygen erosion, which affects objects in Low Earth Orbit (LEO) [5], collisions with micrometeorites and space debris, posing serious risks [6] and radiation exposure, particularly ultraviolet (UV) radiation, that can degrade tether materials and reduce their operational lifespan. Over the years, both manned and unmanned missions have contributed to the progress of research in the field of flexible orbital structures [7].

This study focuses on the stability of Space Tether Cable Systems. The methodology was emphasized through a mathematical model which illustrates a ponderous flexible tether between two point masses.

Hamilton canonical equations complete the numerical analysis by obtaining the final form for the differential equations. The materials used were Kevlar fibre type 49 and Stainless Steel type 316L, considering their mechanical properties.

The configurations were analysed in a MATLAB program using the ODE (Ordinary differential equations) functions: ODE45 and ODE15S.

Conclusions were drawn after identifying the most stable configuration of a Space Tether Cable System.

2. METHODOLOGY

Mathematical models of space tether systems describe the dynamic behaviour of the entire assembly, taking into account orbital, gravitational, electrodynamic and mechanical influences. These models are essential for the design, the control, and the stability analysis of the STS.

2.1 Simple model of a spatial tether system consisting of two material points connected by a tether

The simplest model of tether system are those that represent the tether as a massless bar, a common approach in the early studies of STS dynamics. Their simplicity makes it possible to identify key qualitative features of STS motion using relatively straightforward methods. Additionally, these models are frequently used for preliminary or approximate calculations [1].

2.1.1 Model of an STS with a massive flexible tether

Numerous studies in STS dynamics [8] [9] describe such systems using a model consisting of two point masses connected by a tether with considerable mass. A mechanical system consisting of two particles, A and B, connected by a tether (AB) operating within Earth's gravitational field is considered (Fig. 1).

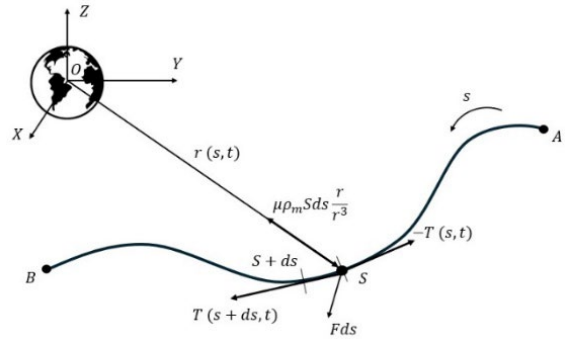

Fig. 1 STS consisting of two point masses connected by a flexible tether [1]

Firstly, an elemental section of the tether, ds, with density $\rho_M(s)$ and cross-sectional area S is isolated. Tension forces act on this section from the adjacent parts of the tether: $\mathbf{T}(s+ds,t)$ from the s towards B, and $-\mathbf{T}(s,t)$ from the s towards A. $\mathbf{r}(s,t)$ is denoted as the position vector of point s at time t. Within a fixed geocentric coordinate system OXYZ, Newton's equation for the centre of mass of this section can be written as:

$$\rho_M(s)ds\frac{\partial^2\mathbf{r}}{\partial t^2}S = \mathbf{T}(s+ds,t) - \mathbf{T}(s,t) - \rho_M(s)\mu ds\frac{\mathbf{r}}{r^3}S + \mathbf{F}ds \tag{1}$$

where **F** is the vector of the intensity of external forces.

Given the previous equation, the following expression is obtained:

$$\rho_M\frac{\partial^2\mathbf{r}}{\partial t^2}S = \frac{\partial\mathbf{T}}{\partial s} - \rho_M S\mu\frac{\mathbf{r}}{r^3} + \mathbf{F} \tag{2}$$

Equation (2) represents the dynamic equation of the massive flexible tether. Due to its flexibility, the tension force in the tether is always directed along the local tangent to its axis and is determined by Hooke's law:

$$\mathbf{T} = ES(\gamma-1)\boldsymbol{\tau} \tag{3}$$

where E is the modulus of elasticity; $\gamma = \left|\frac{\partial\mathbf{r}}{\partial s}\right|$ is the unit elongation of the tether section and $\boldsymbol{\tau} = \left(\frac{\partial\mathbf{r}}{\partial s}\right)\left|\frac{\partial\mathbf{r}}{\partial s}\right|^{-1}$ is the unit vector, tangential to the line of the tether.

By introducing the terms of the Hooke's law in the second equation, the new equation is:

$$\rho_M\frac{\partial^2\mathbf{r}}{\partial t^2} = \frac{\partial}{\partial s}\left[ES\frac{\partial\mathbf{r}}{\partial s}\left(1-\left|\frac{\partial\mathbf{r}}{\partial s}\right|^{-1}\right)\right] - \rho_M\mu\frac{\mathbf{r}}{r^3}S + \mathbf{F} \tag{4}$$

The vector partial differential equation of the wave type is defined over a domain with variable boundaries. The boundary conditions are given by the motion equations of the end bodies:

$$\begin{aligned} m_A(t)\frac{d^2\mathbf{r}_A}{dt^2} &= \boldsymbol{\tau}_A\left[T_A - \rho_M(s_A)\gamma_A\left(\frac{ds_A}{dt}\right)^2 S\right] - m_A(t)\mu\frac{\mathbf{r}_A}{r_A^3} + \mathbf{F}_A, \\ m_B(t)\frac{d^2\mathbf{r}_B}{dt^2} &= -\boldsymbol{\tau}_B\left[T_B - \rho_M(s_B)\gamma_B\left(\frac{ds_B}{dt}\right)^2 S\right] - m_B(t)\mu\frac{\mathbf{r}_B}{r_B^3} + \mathbf{F}_B \end{aligned} \tag{5}$$

Mounting points of the tether A_k and B_k are used instead of points A and B, which represent the mass centres of the bodies, if within the limits, the model of the rigid bodies at the tips of the tether is considered in the (4) equation.

The dynamic equations of motion of the end bodies regarding their centres of mass are:

$$\begin{aligned} \|I_A\|\dot{\boldsymbol{\omega}}_A &= -\boldsymbol{\omega}_A \times \|I_A\| \cdot \boldsymbol{\omega}_A + \mathbf{d}_A \times \boldsymbol{\tau}_{A_k} T_{A_k} + 3\frac{\mu}{r_A^3}\boldsymbol{\tau}_A \times \|I_A\|\boldsymbol{\tau}_A + \mathbf{M}_A, \\ \|I_B\|\dot{\boldsymbol{\omega}}_B &= -\boldsymbol{\omega}_B \times \|I_B\| \cdot \boldsymbol{\omega}_B + \mathbf{d}_B \times \boldsymbol{\tau}_{B_k} T_{B_k} + 3\frac{\mu}{r_B^3}\boldsymbol{\tau}_B \times \|I_B\|\boldsymbol{\tau}_B + \mathbf{M}_B \end{aligned} \tag{6}$$

where $\|I_A\|$, $\|I_B\|$ are the matrix of the tensors of inertia of the end bodies; $\boldsymbol{\omega_A}$, $\boldsymbol{\omega_B}$ are the vectors of the absolute angular velocities concerning the centre of mass; $\mathbf{d}_A, \mathbf{d}_B$ are vectors of the defining position of the tether mounting points concerning the centre of mass; $\mathbf{M}_A$, $\mathbf{M}_B$ are moments of external forces; and $\boldsymbol{\tau}_i = \left(\frac{\partial \mathbf{r}_i}{\partial s}\right)\left|\frac{\partial \mathbf{r}_i}{\partial s}\right|^{-1}$.

The following equations describe the motion of points A_k and B_k:

$$\begin{aligned} \ddot{\mathbf{r}}_{A_k} &= \ddot{\mathbf{r}}_A + \boldsymbol{\omega}_A \times \mathbf{d}_{A_k} + \boldsymbol{\omega}_A \times (\boldsymbol{\omega}_A \times \mathbf{d}_{A_k}), \\ \ddot{\mathbf{r}}_{B_k} &= \ddot{\mathbf{r}}_B + \boldsymbol{\omega}_B \times \mathbf{d}_{B_k} + \boldsymbol{\omega}_B \times (\boldsymbol{\omega}_B \times \mathbf{d}_{B_k}), \end{aligned} \tag{7}$$

where $\mathbf{r}_{A_k}, \mathbf{r}_{B_k}$ are the position vectors of the mounting points in the coordinate system.

The model exhibits singularities regardless of whether the spatial motion of rigid bodies is considered or not. The key singularity arises from the fact that the order of derivatives in the boundary conditions matches that of the partial differential equation. As a result, implementing numerical integration algorithms for this equation is difficult. The requirement for a very small time integration step, Δt is very strict. This step size is determined by the propagation speed of longitudinal oscillations along the tether, denoted as v_E.

$$\Delta t < \frac{\Delta s}{v_E} = \frac{\Delta s}{\sqrt{ES/\rho_M}} \tag{8}$$

where Δs is the distance between mesh nodes.

2.2 Hamilton's Canonical Equations

To perform a comprehensive stability analysis in the Earth's orbit, the Hamiltonian formulation is utilized to generate the first-order differential equations. The Hamiltonian exhibits a hybrid form, being both a function and a functional [10]:

$$H = \sum_{i=1}^{3} \frac{\partial L}{\partial \dot{\theta}_i}\dot{\theta}_i + \int_{D_e}\left(\frac{\partial \hat{L}}{\partial \dot{u}_c}\dot{u}_c + \frac{\partial \hat{L}}{\partial \dot{v}_c}\dot{v}_c + \frac{\partial \hat{L}}{\partial \dot{w}_c}\dot{w}_c\right)dD_e - L \tag{9}$$

D_e is the domain occupied by the body in undeformed state [10]. The momenta considered are:

$$\begin{aligned} p_{\theta_i} &= \frac{\partial L}{\partial \dot{\theta}_i}, \qquad i = 1,2,3 \\ \hat{p}_{u_c} &= \frac{\partial \hat{L}}{\partial \dot{u}_c}, \hat{p}_{v_c} = \frac{\partial \hat{L}}{\partial \dot{v}_c}, \hat{p}_{w_c} = \frac{\partial \hat{L}}{\partial \dot{w}_c} \end{aligned} \tag{10}$$

The momentum densities are illustrated in the new Hamiltonian expression:

$$H = \sum_{i=1}^{3} p_{\theta_i}\,\dot{\theta}_i + \int \left(\hat{p}_{u_c}\dot{u}_c + \hat{p}_{v_c}\dot{v}_c + \hat{p}_{w_c}\dot{w}_c\right) dD_e - L$$

$$= \int_{D_e} \hat{H}\left(\begin{matrix}\theta_i, u_c, v_c, w_c, p_{\theta_i}, \hat{p}_{u_c}, \hat{p}_{v_c}, \hat{p}_{w_c},\\ \frac{\partial u_c}{\partial x}, \frac{\partial v_c}{\partial y}, \dots, \frac{\partial w_c}{\partial z}, \frac{\partial^2 u_c}{\partial x^2}, \frac{\partial^2 u_c}{\partial x \partial y}, \dots, \frac{\partial^2 w_c}{\partial z^2}\end{matrix}\right) dD_e \tag{11}$$

where $\hat{H}$ is the Hamiltonian density.

The variation of the Hamiltonian is expressed by accounting for both forms presented in equation (11).

After considering the (10) equations and the variation of the Hamiltonian, the Hamiltonian equations are:

$$\dot{\theta}_i = \frac{\partial H}{\partial p_{\theta_i}}, \qquad \dot{p}_{\theta_i} = -\frac{\partial H}{\partial \theta_i}, \qquad i = 1, 2, 3 \tag{12}$$

$$\dot{u}_c = \frac{\partial \hat{H}}{\partial \hat{p}_{u_c}}, \dot{v}_c = \frac{\partial \hat{H}}{\partial \hat{p}_{v_c}}, \dot{w}_c = \frac{\partial \hat{H}}{\partial \hat{p}_{w_c}} \tag{13}$$

Equations (12) and (14) were formulated using Lagrange's equations, the ordinary differential equation for attitude motion and the equation for damping forces.

$$\dot{\hat{p}}_{u_c} = -\frac{\partial \hat{H}}{\partial u_c} + \mathcal{L}_{u_c}[u_c, v_c, w_c] + \hat{Q}_{u_c}$$

$$\dot{\hat{p}}_{v_c} = -\frac{\partial \hat{H}}{\partial v_c} + \mathcal{L}_{v_c}[u_c, v_c, w_c] + \hat{Q}_{v_c} \tag{14}$$

$$\dot{\hat{p}}_{w_c} = -\frac{\partial \hat{H}}{\partial w_c} + \mathcal{L}_{w_c}[u_c, v_c, w_c] + \hat{Q}_{w_c}$$

Equations (13) and (14) must be satisfied at every point of the domain D_e. The domain D_e is bounded by the surface S. The boundary conditions are:

$$B_j[u_c, v_c, w_c] \cdot B_k[u_c, v_c, w_c] = 0 \; on \; S, j = 1, 2; k = 3, 4 \tag{15}$$

The Hamiltonian takes the following form when the kinetic energy is quadratic in the generalized velocities:

$$H = T + V_{EL} \tag{16}$$

where H is the total energy of the system [10].

In order to analyse the stability of the flexible orbital structures, a MATLAB program was used. In the MATLAB program the ordinary differential equations were solved based on methods and formulas for stiff and non-stiff systems.

Runge-Kutta of 4th and 5th order is an adaptive method that automatically adjusts the integration step size to keep the numerical error within a certain limit. It provides error control

using an embedded lower order estimate. It optimizes stability and accuracy by minimizing the truncation error in the 5th order method [11].

This method is appropriate for solving equations with low to moderate stiffness and serves as the basis for the ODE45 solver [12].

Backward differentiation formula (BDF) is an implicit method, which requires solving systems of linear equations at each integration step. BDF ensures numerical stability, making it particularly suitable for stiff problems. BDF methods operate with a nearly constant step size and a variable order, typically reaching up to the 5th or 6th order. The solution at each step is computed using a simplified Newton iteration, initialized with a predictor estimate. The nearby solutions change rapidly, requiring the numerical method to take small steps in order to achieve accurate results [13].

This method is implemented in the ODE15S solver, which utilizes variable-order formulas to adapt its accuracy based on the problem's characteristics, making it effective in cases where methods like ODE45 would need small time steps to maintain stability [12].

The simulation conducted in this study examines the configuration of a massive flexible tether in two scenarios: one using Kevlar fibre type 49 and the other using Stainless Steel type 316L. The materials were selected based on their properties that are suitable for space applications.

Kevlar fibre type 49 is the most commonly used type for space tether applications due to its favourable mechanical and thermal properties. Kevlar fibre type 49 has a tensile strength with a modulus between those of glass and carbon fibres, and it has a lower density than both materials [14]. It has high thermal stability, strong erosion resistance, low creep, is lightweight, ideal for orbital structures and it is five times stronger than steel [15].

Stainless Steel type 316L is used for space tether systems primarily for components where mechanical strength is essential. It offers high corrosion and oxidation resistance, good toughness and ductility [16].

It has strong resistance to radiation, making it suitable for demanding space environments [17]. Austenitic stainless steel is highly weldable due to its low carbon content and can be easily shaped into different forms [18].

3. RESULTS

To perform the simulations in the MATLAB program, it was necessary to establish the initial data. The initial data are highlighted in the table below:

Table 1. Initial data

Initial data	Description	Value
$R_p\ [m]$	Earth Radius	6.371e+6
$GME\ [m^3/s^2]$	Earth's gravitational constant	3.98e+14
$H\ [m]$	Orbital altitude	45e+4
$Omega\ [rad/s]$	Rotation speed	-1.12e-3
$V_{cm}\ [m/s]$	Centre of mass speed	7644.43
$T\ [s]$	Duration of an orbit	5606
$Time\ [s]$	Simulation duration	5000
ODE45 or ODE15S	Solver	-

For each configuration, the following are defined:

- Number of points (nodes), point coordinates ($X\,[m], Y[m]$), mass for each point ($Mass\,[kg]$)
- Elasticity constants ($K_e\,[N/m]$) and damping constants ($K_a\,[N/(\frac{m}{s})]$) for the cables connecting the points

The program displays the start configuration and the evolution of the elongation in time for each simulation. The trajectory of the tether in Earth's orbit is also illustrated.

The configuration consists of a 200 km cable divided into segments of 10 km each. Each section is defined by two mass points, with each mass point weighing 1,000 kg for Kevlar fibre type 49 and 400 kg for Stainless Steel type 316L.

The mass points located at the ends of the cable for both materials weigh 10,000 kg each, resulting in a massive tether system.

The cable's elasticity and damping constants vary depending on the material used. For Kevlar fibre type 49 the elasticity constant is 10 kN/m and the damping constant is 20 $\mathrm{N}/(\frac{\mathrm{m}}{\mathrm{s}})$. In contrast, Stainless Steel type 316L the elasticity constant is 20 kN/m and the damping constant is 2 $\mathrm{N}/(\frac{\mathrm{m}}{\mathrm{s}})$.

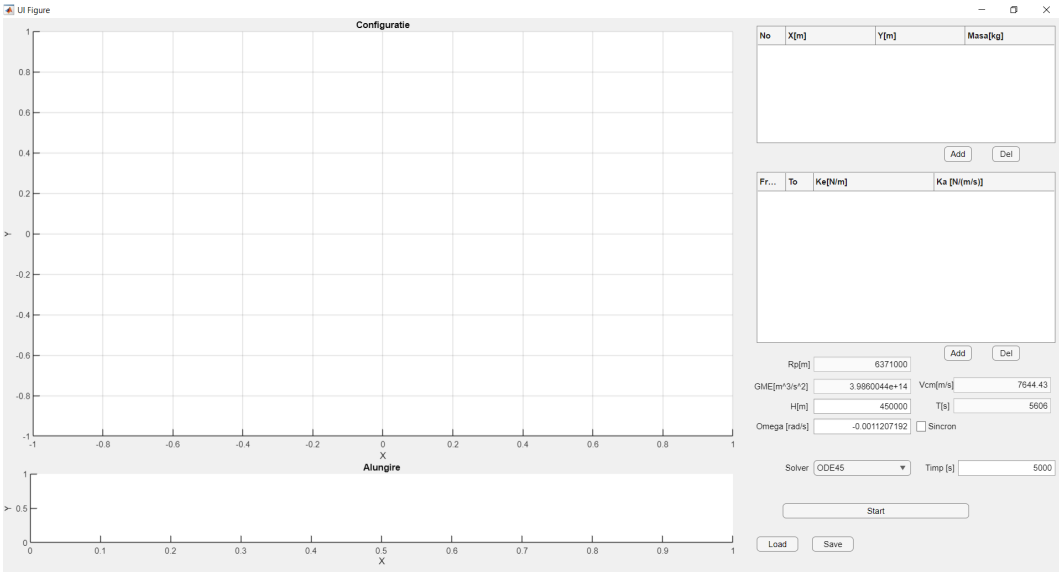

Fig. 2 Program interface

I. Kevlar type 49

The first case study examines a long tether in Low Earth Orbit (LEO), rotating around its centre of mass. The substantial length of the cable introduces orbital perturbations caused by the gravitational gradient.

In the case of Kevlar, its relatively high damping contributes to the passive stability of the system. However, due to the discontinuities in the equations that arise when the cable transitions between tensioned and loose states, a stiff numerical integration method is required. The accurate numerical solution is provided by the stiff solver, as evidenced by the segment elongation plots shown in the two figures (Fig. 4 and Fig. 5).

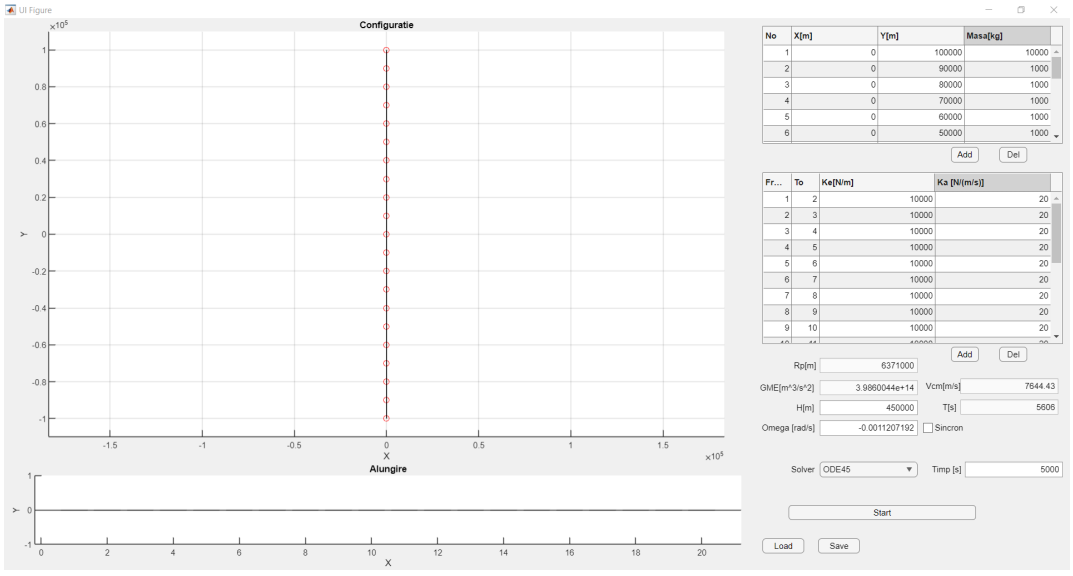

Fig. 3 Start configuration

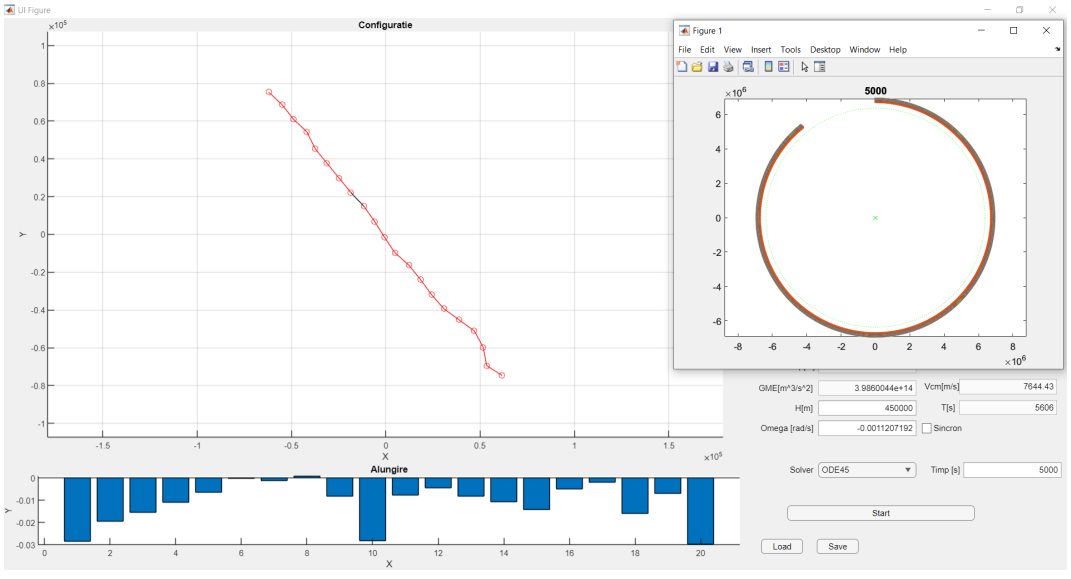

Fig. 4 Partially unstable configuration for ODE45

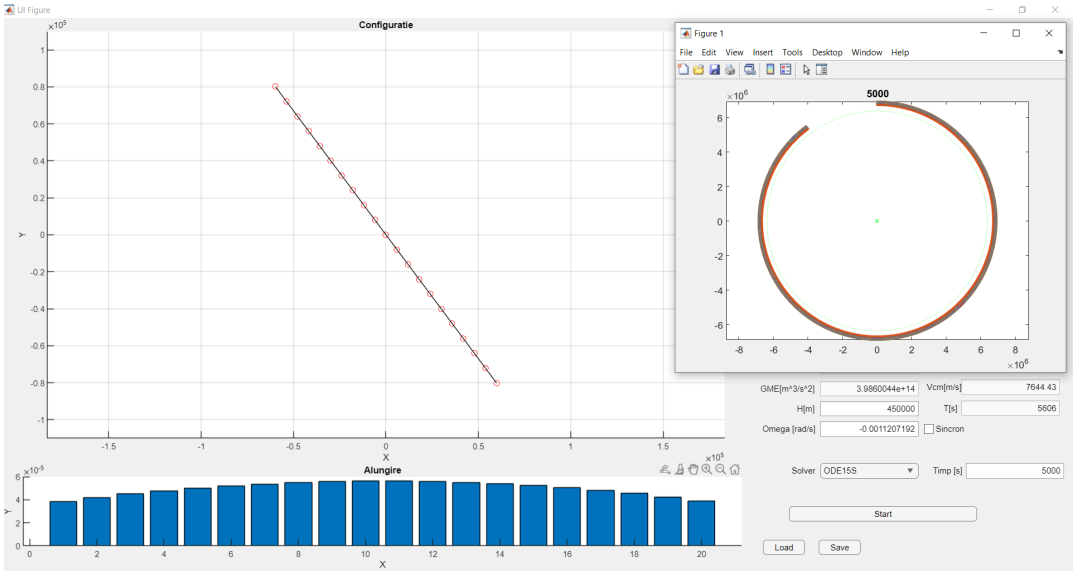

Fig. 5 Stable configuration for ODE15S

II. Stainless Steel type 316L

For Stainless Steel, the combination of the cable's relatively high mass and low damping constant results in critical numerical instability when using the 4th order Runge-Kutta method. Nevertheless, the equations remain solvable using a stiff integration method (Fig. 8).

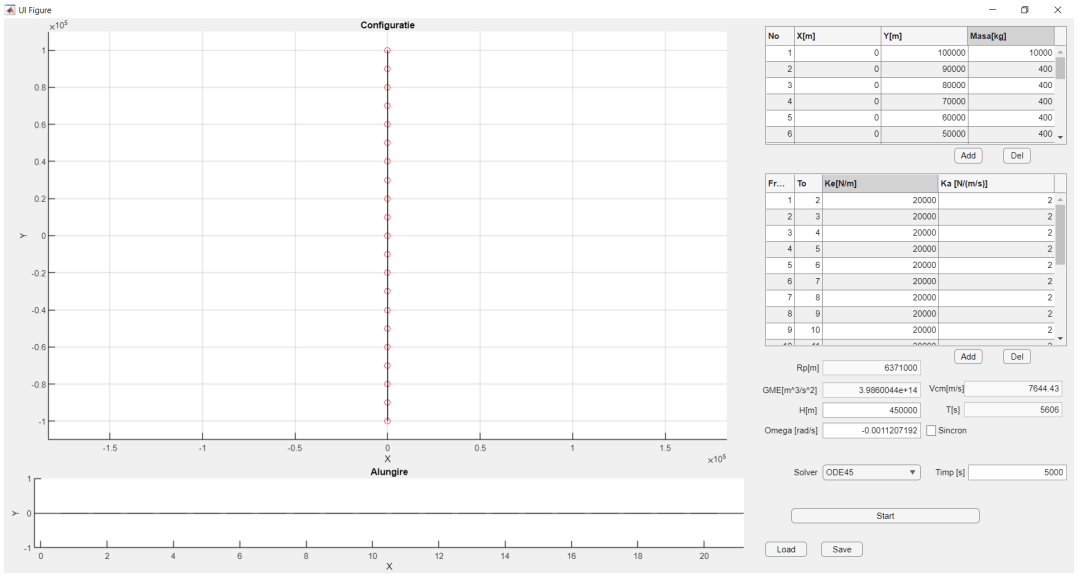

Fig. 6 Start configuration

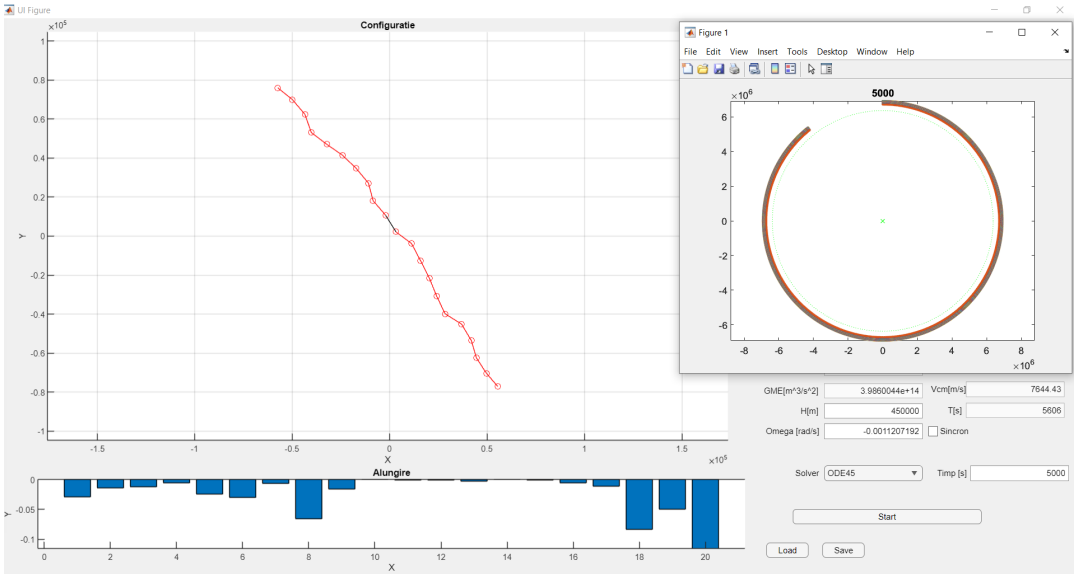

Fig. 7 Unstable configuration for ODE45

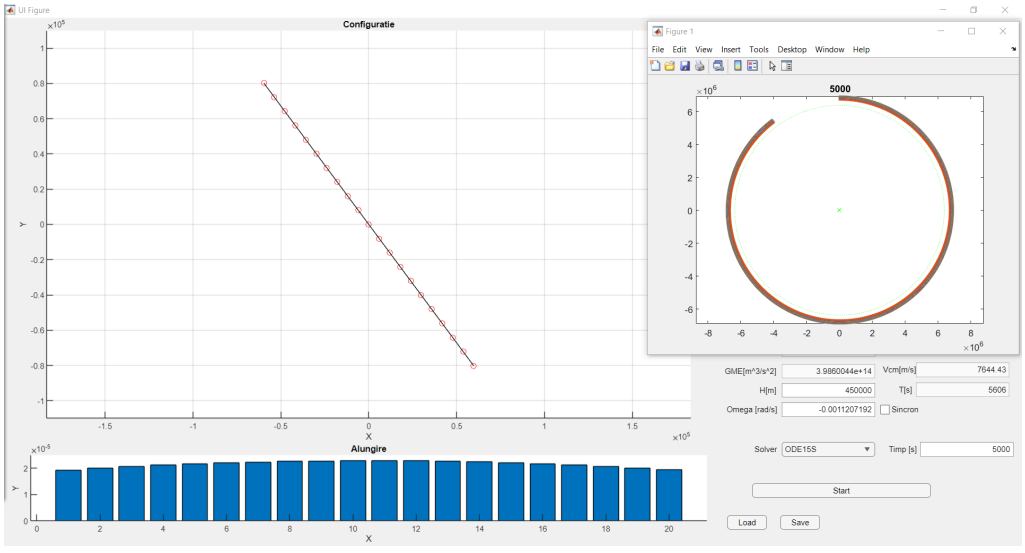

Fig. 8 Stable configuration for ODE15S

4. CONCLUSIONS

The stability of space tether systems is a key factor in the study of tether propulsion and orbital dynamics. Tether length influences dynamic stability, excessive cable length can lead to increased system instability.

Although a high damping coefficient is necessary to maintain stability, it also causes greater energy loss. Since this energy is essential for the satellite's successful orbital insertion, its dissipation can result in a decreased altitude relative to Earth, which is an unfavourable outcome.

The experimental and numerical analysis of space tether systems yielded several important insights regarding material behaviour, numerical methods and configuration complexity.

Kevlar-based configuration demonstrated superior performance in simulations due to Kevlar's high tensile strength and low weight, making it well-suited for flexible orbital structures where stability is important.

In contrast, Stainless Steel, while offering greater resistance to corrosion and extreme temperatures, showed increased susceptibility to instability, which induces significant dynamic imbalances and substantial oscillations.

Among the numerical solvers evaluated, ODE45 was found to be effective for problems with low stiffness, providing a good balance between computational efficiency and solution accuracy. In contrast, ODE15S proved to be more suitable for stiff problems, including complex structural layouts, offering enhanced numerical stability and minimizing errors associated with stiff differential equations.

This study of stability of flexible orbital structures emphasizes the need for optimization in the number and arrangement of nodes and connections to mitigate stress accumulation and structural deformation.

REFERENCES

[1] V. S. Aslanov and A. S. Ledkov, *Dynamics of tethered satellite systems*, Woodhead Publishing Limited, 2012.

[2] E. C. Lorenzini, R. D. Estes and M. Cosmo, In-Space Transportation with Tethers, *NASA Technical Reports*, 1999.

[3] M. Tinker, T. Bryan, J. Vaughn, J. D. Hunter, S. Canfield, B. Hargis and J. MacArthur, Electric Sail Tether Deployment System for CubeSats, in *IEEE Aerospace Conference*, Big Sky, 2021.

[4] J. Pearson, E. M. Levin, J. Caroll and J. C. Oldson, Orbital Maneuvering with Spinning Electrodynamic Tethers, *American Institute of Aeronautics and Astronautics,* 2004.

[5] K. d. Groh, B. A. Banks and R. Demko, Techniques for Measuring Low Earth Orbital Atomic Oxygen Erosion of Polymers, *NASA Technical Reports,* 2002.

[6] A. S. L. V. S. Aslanov, Survey of tether system technology for space debris removalmissions, *Journal of Spacecraft and Rockets,* vol. **60**, pp. 1355-1371, 2023.

[7] E. C. L. G. Sanchez-Arriaga and S. G. Bilen, A Review of Electrodynamic Tether Missions: Historical Trend, Dimensionless Parameters, and Opportunities Opening Space Markets, *Acta Astronautica,* 2024.

[8] Y. Ahn, W. Jang, J. Lee and J. Chung, Dynamic Analysis of Tethered Satellites with a Payload Moving Along a Flexible Tether, *Applied sciences,* 2024.

[9] W. Jung, A. P. Mazzoleni and J. Chung, "Dynamic analysis of a tethered satellite system, *Nonlinear Dynamics,* 2014.

[10] L. Meirovitch and R. A. Calico, *The stability of motion of satellites with flexible appendages*, NASA, Cincinnati, 1972.

[11] J. R. Dormand and P. J. Prince, A family of embedded Runge-Kutta formulae, *Journal of Computational and Applied Mathematics,* vol. **6**, pp. 19-26, 1980.

[12] L. F. Shampine and M. W. Reichelt, The MATLAB ODE Suite, *SIAM Journal on Scientific Computing,* vol. **18**, pp. 1-22, 1997.

[13] L. F. Shampine, M. W. Reichelt and J. A. Kierzenka, Solving Index-1 DAEs in MATLAB and Simulink, *SIAM Review,* vol. **41**, pp. 538-552, 1999.

[14] K. K. H. Yeung and K. P. Rao, Mechanical Properties of Kevlar-49 Fibre Reinforced ThermoplasticComposites, *Polymers & Polymer Composites,* vol. **20**, 2012.

[15] F. J. Khusiafan, Use of KEVLAR® 49 in Aircraft Components, *Engineering Management Research,* vol. **7**, 2018.

[16] A. M. Philip and K. Chakraborty, Some studies on the machining behaviour of 316L austenitic stainless steel, *materialstoday: PROCEEDINGS,* vol. **56**, pp. 681-685, 2022.

[17] P. B. R. Rajan, I. Monnet, E. Hug, A. Etienne, N. Enikeev, C. Keller, X. Sauvage, R. Z. Valiev and B. Radiguet, Irradiation resistance of a nanostructured 316 austenitic stainless steel, *IOP Conference Series Materials Science and Engineering,* 2014.

[18] K. Kanlayasiri, T. Khuenkaew, P. Sangrayub and P. Jattakul, Assessment of resistance spot welding parameters on the strength and reliability of AISI 316L stainless steel joints, *Creative Science,* 2025.